Chemistry & Biology
Article

Discovery of Specific Inhibitors of Human USP7/HAUSP Deubiquitinating Enzyme

Céline Reverdy,[1,4] Susan Conrath,[1,4] Roman Lopez,[1] Cécile Planquette,[1] Cédric Atmanene,[2] Vincent Collura,[1] Jane Harpon,[1] Véronique Battaglia,[1] Valérie Vivat,[2] Wolfgang Sippl,[3] and Frédéric Colland[1,*]
[1]Hybrigenics Pharma, 3-5 Impasse Reille, 75014 Paris, France
[2]NovAliX, Bioparc, Boulevard Sebastien Brant, 67400 Illkirch, France
[3]Institute of Pharmaceutical Chemistry, Martin-Luther-University Halle-Wittenberg, Wolfgang-Langenbeck-Str. 4, 06120 Halle (Saale), Germany
[4]These authors contributed equally to this work
*Correspondence: fcolland@hybrigenics.com
DOI 10.1016/j.chembiol.2012.02.007

SUMMARY

The human USP7 deubiquitinating enzyme was shown to regulate many proteins involved in the cell cycle, as well as tumor suppressors and oncogenes. Thus, USP7 offers a promising, strategic target for cancer therapy. Using biochemical assays and activity-based protein profiling in living systems, we identified small-molecule antagonists of USP7 and demonstrated USP7 inhibitor occupancy and selectivity in cancer cell lines. These compounds bind USP7 in the active site through a covalent mechanism. In cancer cells, these active-site-targeting inhibitors were shown to regulate the level of several USP7 substrates and thus recapitulated the USP7 knockdown phenotype that leads to G1 arrest in colon cancer cells. The data presented in this report provide proof of principle that USP7 inhibitors may be a valuable therapeutic for cancer. In addition, the discovery of such molecules offers interesting tools for studying deubiquitination.

INTRODUCTION

Deregulation of the ubiquitin-proteasome system has been implicated in the pathogenesis of many human diseases, including cancer. The effectiveness of the proteasome inhibitor Velcade (bortezomib) in the treatment of multiple myeloma and mantle cell lymphoma establishes the ubiquitin-proteasome system as a valid anti-cancer therapeutic target (Cohen and Tcherpakov, 2010). Mono- and polyubiquitination can be reversed by deubiquitinating enzymes (DUBs), which specifically cleave the isopeptide bond at the C terminus of ubiquitin (Komander et al., 2009; Nijman et al., 2005). USP proteins constitute the largest subfamily of DUBs, with more than 60 human members. These enzymes remove ubiquitin from specific protein substrates, making it possible to retrieve these proteins from proteasomal degradation and alter their location and activation (Komander et al., 2009; Nijman et al., 2005). Based on their protease activity and involvement in several human diseases, USPs are emerging as potential targets for pharmacological disruption of the ubiquitin regulation machinery (Colland, 2010; Drag and Salvesen, 2010).

USP7/HAUSP (herpes virus-associated USP) is a 135 kDa protein in the USP family of DUB enzymes. In addition to a DUB domain, USP7 also contains an N-terminal TRAF-like MATH domain (Zapata et al., 2001) and a C-terminal domain that contains at least five ubiquitin-like domains (Faesen et al., 2011). This protein is produced ubiquitously and is highly conserved in eukaryotes. USP7 is primarily a nuclear protein and localizes to a subset of PML bodies (Everett et al., 1999; Muratani et al., 2002). At the molecular level, by virtue of its deubiquitinating activity, USP7 has been shown to regulate the steady-state level of several poly-ubiquitinated substrates. For example, USP7 alters the level of the p53 and $p16^{INK4a}$ tumor suppressors through Mdm2 stabilization and Bmi1/Mel18 stabilization, respectively (Cummins et al., 2004; Li et al., 2004; Maertens et al., 2010). USP7 binding to p53 was recently shown to be regulated by TSPYL5, a protein potentially involved in breast oncogenesis through its competition with p53 for binding to the same region of USP7 (Epping et al., 2011). Additional proteins involved in genomic integrity and regulation, such as the DNMT1 DNA methylase and the claspin adaptor, are also stabilized by USP7 (Du et al., 2010; Faustrup et al., 2009). Interestingly, USP7 was shown to regulate the cellular compartmentalization of several mono-ubiquitinated substrates by deubiquitination. In this respect, the PTEN and FOXO4 tumor suppressors are inactivated by USP7-induced nuclear export (Song et al., 2008; van der Horst et al., 2006). USP7 overexpression was also reported in human prostate cancer and was directly associated with tumor aggressiveness (Song et al., 2008). Previous in vivo data also underlined the involvement of USP7 in cancer cell proliferation (Becker et al., 2008). Altogether, the phenotypes associated with USP7-silencing, as well as the connections between USP7 and several pathways involving oncogenes and tumor suppressors, strongly suggest that targeting USP7 by small-molecule inhibitors may be of therapeutic value in cancer treatment.

We developed advanced high-throughput screening-compatible assays using optimized USP substrates, including various ubiquitin derivatives and specific physiological substrates, to screen a chemically diverse library of small molecules. From a pioneering program, HBX 41,108 was found to inhibit USP7

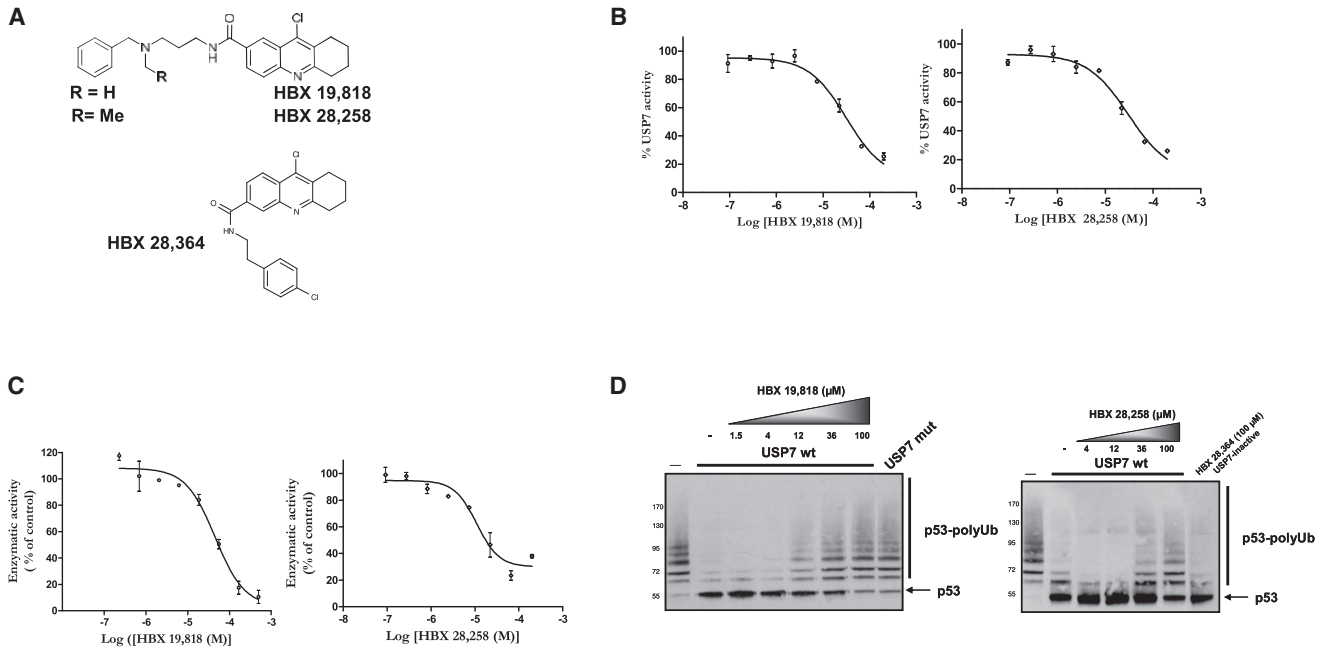

Figure 1. Identification of HBX 19,818 and HBX 28,258 as USP7 Inhibitors

(A) Structures of the amidotetrahydroacridine derivatives HBX 19,818, HBX 28,258, and HBX 28,364.

(B) Dose-dependent inhibition of USP7 activity by HBX 19,818 and HBX 28,258 using the Ub-AMC substrate. The results are shown as means ± SD of triplicate values and are representative of four independent experiments.

(C) Dose-dependent inhibition of USP7 activity by HBX 19,818 and HBX 28,258 using the Ub-52 substrate. The results are shown as means ± SD of triplicate values and are representative of four independent experiments.

(D) HBX 19,818 and HBX 28,258 inhibit USP7 deubiquitination of polyubiquitinated p53. The purified wild-type or mutant (C223A) USP7 enzyme (3 nM final concentration) was incubated with HBX 19,818 (1.5, 4, 12, 36, or 100 μM), HBX 28,258 (4, 12, 36, or 100 μM), or HBX 28,364 (100 μM) for 1 hr at room temperature before the addition of purified polyubiquitinated p53 and incubation for 1 hr at 37°C. The results are representative of two independent experiments.

deubiquitinating activity with submicromolar IC_{50} and affect USP7-mediated p53 deubiquitination in vitro and in cells. Like RNAi-mediated USP7 silencing in cancer cells, HBX 41,108 treatment stabilized p53, activated the transcription of a p53 target gene, and inhibited cancer cell growth (Colland et al., 2009). One of the main problems hindering the development of small-molecule inhibitors of cysteine proteases has been their lack of specificity (Altun et al., 2011). Work carried out over the last few years has led to the identification of inhibitors with selective action against various DUB targets demonstrating the feasibility of selectively targeting deubiquitinating enzymes. The PLPro-specific inhibitors (Ratia et al., 2008), the USP14-specific inhibitors (Lee et al., 2010), and the USP1-specific inhibitors (Chen et al., 2011) are three such examples. We describe here the identification of selective small-molecule antagonists of USP7 that bind in its active site through a covalent mechanism. In cellular models, these active-site targeting inhibitors were shown to bind directly and specifically to USP7 and modulate the steady-state levels of several USP7 substrates.

RESULTS

Identification of USP7-Small Molecule Inhibitors

To identify USP7 inhibitors, we performed an in vitro high-throughput screen (HTS) against a diverse library of synthetic chemicals using ubiquitin C-terminal 7-amido-4-methylcoumarin (Ub-AMC) as a substrate (Dang et al., 1998). Full-length USP7 protein was produced as a functional enzyme in baculovirus-infected insect cells and purified using a His-tag fusion method as previously described (Colland et al., 2009). The Z and Z' factors, which are standard statistical parameters for HTS assays, were 0.76 and 0.92, respectively, confirming HTS assay robustness (Zhang et al., 1999). From this screening, we discovered a structural class of small molecules represented by HBX 19,818 and HBX 28,258 (Figure 1A). These compounds inhibited USP7 activity with IC_{50} of 28.1 and 22.6 μM, respectively (Figure 1B). We obtained similar IC_{50} for these compounds using an assay based on another substrate, the natural ubiquitin precursor Ub52, which confirmed the efficacy of each compound (Figure 1C). We sought to confirm this finding using a more physiological USP7 substrate, polyubiquitinated p53 (polyUb-p53), which we generated in vitro using the ubiquitin ligase Mdm2 as previously described (Colland et al., 2009). Wild-type USP7—but not the catalytically inactive C223A mutant—deubiquitinated the polyUb-p53 substrate (Figure 1D). We then assessed the effects of HBX 19,818 and HBX 28,258 on USP7-mediated p53 deubiquitination and showed that both molecules exhibited a dose-dependent effect on USP7 activity (Figures 1A and 1D). In contrast, a related inactive compound, HBX 28,364, devoid of the basic alkyl amine side chain, did not exhibit any inhibitory activity (Figures 1A and 1D). This new structural class of small molecules is thus able to inhibit

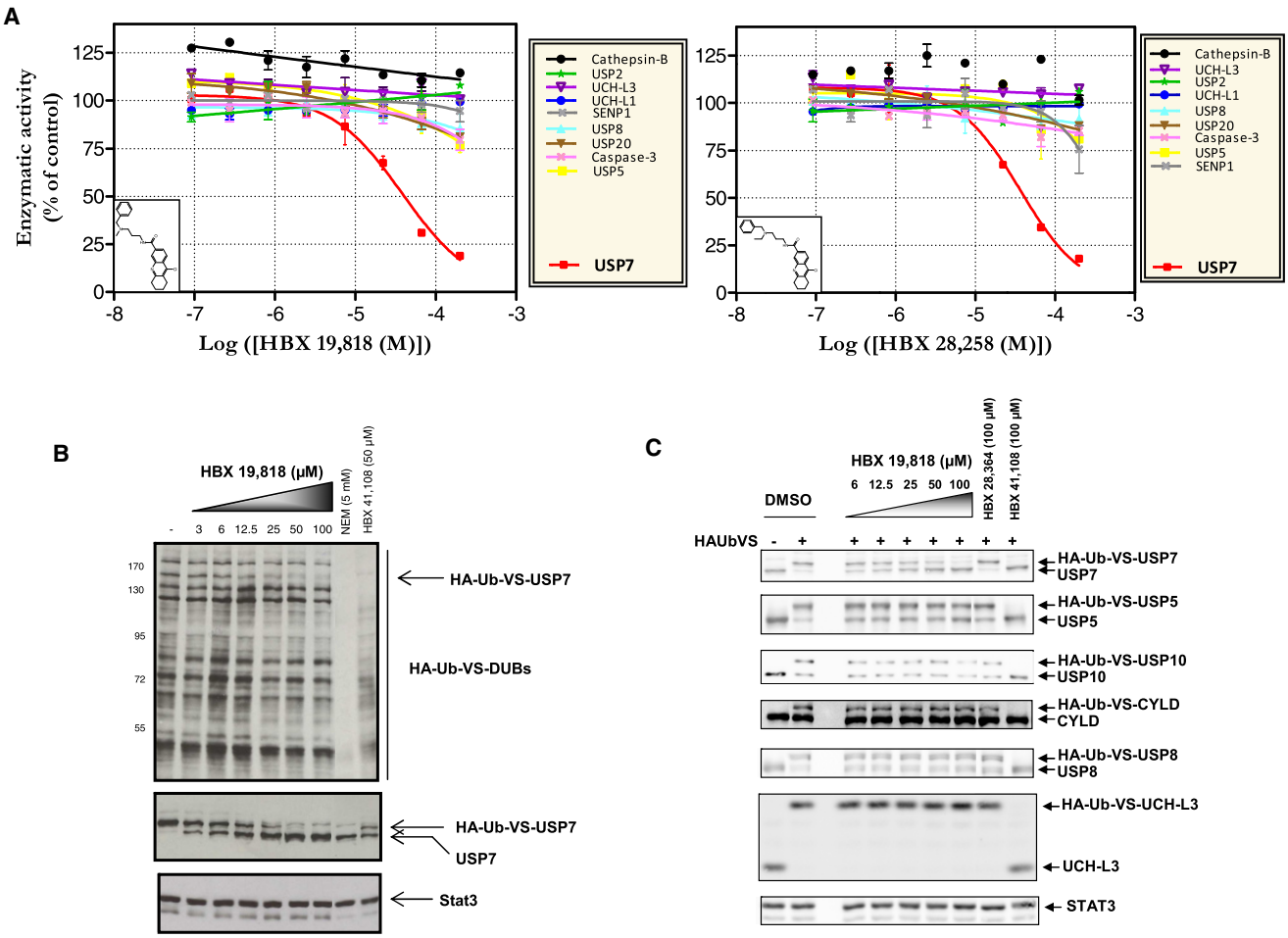

Figure 2. HBX 19,818 and HBX 28,258 Selectively Inhibit USP7

(A) A panel of ten representative active cysteine proteases was established to evaluate the specificity of HBX 19,818 and HBX 28,258 in vitro.

(B) This panel shows a gel from a HAUbVS competition assay for HBX 19,818 (3, 6, 12.5, 25, 50, and 100 μM), NEM (5 mM), and HBX 41,108 (50 μM) with the HCT116 proteome. All active DUBs were identified using anti-HA antibody. Note that HBX 19,818 blocks only USP7 and not the other deubiquitinating enzymes.

(C) HAUbVS competition assay gels comparing the activity of HBX 19,818, HBX 28,364, and HBX 41,108 inhibitors against USP7 and additional deubiquitinating enzymes (USP8, USP5, USP10, CYLD, and UCH-L3) in native HCT116 cell lysate. HBX 19,818 exhibits specific and concentration-dependent inhibition of USP7 labeling by HAUbVS in the HCT116 proteome.

See also Figures S1 and S2.

USP7-mediated deubiquitination of artificial, as well as physiologically relevant, substrates.

Selectivity of the Small-Molecule Inhibitors of USP7

We evaluated the specificity of HBX 19,818 and HBX 28,258 for USP7 relative to other proteases by assessing the inhibitory effects of these compounds in vitro against a representative set of recombinant proteases. Interestingly, neither compound exhibited any cross-reactivity on other USP members, such as USP8, USP5, USP2, and USP20 (IC_{50} > 200 μM; Figure 2A). We also assessed the specificity of HBX 19,818 and HBX 28,258 for USP7 by assessing their activities on two related deubiquitinating enzymes, UCH-L1 and UCH-L3 (ubiquitin C-terminal hydrolase-L1 and L3), and on SENP1, a SUMO protease. Both compounds were inactive against these ubiquitin and ubiquitin-like proteases (IC_{50} > 200 μM). As USP7 is a thiol protease, we also investigated the effects of these inhibitors on other proteases from this family. Neither compound had any significant activity against cathepsin B and caspase-3 (Figure 2A). Evaluation of HBX 19,818 and HBX 28,258 at inhibitor concentrations up to 1 mM confirmed these findings (Figure S1 available online), thus showing that inhibition of these compounds is at least 30-fold more stronger with USP7 than with the other enzymes tested.

To confirm the specificity observed in vitro using recombinant enzymes, we performed competition assays using the HAUbVS activity-based probe (ABP), which binds covalently to the cysteine active site of deubiquitinating enzymes (Borodovsky et al., 2002; Hemelaar et al., 2004; Ovaa et al., 2004). Compared to in vitro assays of individual recombinant enzyme activity, the HAUbVS assay has the advantage of being able to evaluate the effects of inhibitors against numerous deubiquitinating enzymes in native proteomes directly and in parallel, through western blotting with anti-HA antibody. In this assay, an inhibitor

is added to total cell lysate, and the inhibition of various enzymes is determined by labeling the residual active deubiquitinating enzymes with the HAUbVS. When lysed HCT116 cells were treated with HAUbVS in the absence and presence of the nonspecific DUB inhibitor HBX 41,108 (Figures 2B, S2A, and S2B), a strong reduction of the labeling of most active DUBs was observed. Interestingly, in the presence of HBX 19,818, the immunoblot pattern remained largely unchanged with the exception of one band, at the size corresponding to HA-Ub-VS-USP7, which was almost completely eliminated at the higher doses of HBX 19,818 (Figure 2B). This effect of HBX 19,818 on USP7 activity was confirmed using an anti-USP7 antibody as indicated by the mobility shift observed between the treated and nontreated samples (Figures 2B and 2C). We confirmed these findings by testing the activity of HBX 19,818 in a different proteome and by testing the second compound, HBX 28,258 (Figures S2A and S2C).

We next evaluated the effect of USP7 inhibitors on HAUbVS labeling efficiency by monitoring several deubiquitinating enzymes individually. To this end, we used specific antibodies to assess the labeling efficiency of HAUbVS for USP7, USP8, USP5, USP10, CYLD, and UCH-L3 from HCT116 cell lysates. Labeling was confirmed with all tested DUBs, as indicated by the mobility shifts observed between the HAUbVS-treated and nontreated samples albeit with different levels of efficiency (Figure 2C, lanes 1 and 2). We then evaluated HBX 19,818, the nonspecific DUB inhibitor HBX 41,108, and the inactive compound HBX 28,364 for their ability to inhibit the labeling of these DUBs by HAUbVS. As expected, we found that HBX 41,108 inhibited the labeling of all DUBs tested, whereas HBX 28,364 did not exhibit any inhibitory activity (Figure 2C). In contrast, HBX 19,818 efficiently blocked labeling of USP7 but not that of USP8, USP5, USP10, CYLD, or UCH-L3, showing this compound's specificity for USP7 over a panel of active DUBs under physiological conditions (Figure 2C). Taken together, these results indicate that HBX 19,818 and HBX 28,258 are selective inhibitors of the human USP7 enzyme.

Mode of Action of USP7-Selective Small Molecule Inhibitors

Complexes involving USP7 and HBX 19,818 were characterized by electrospray ionization mass spectrometry (ESI-MS) under nondenaturing conditions. Increasing concentrations of HBX 19,818 (one to ten molar equivalents) were incubated with purified USP7(K208-E560), and complex formation was subsequently monitored by native MS. HBX 19,818 was shown to form stoichiometric complex with USP7, which proportion gradually increased with compound concentration, reaching about 80% in the presence of ten molar equivalents (Figure 3A). Only a 1:1 protein/ligand complex was detected in spite of large excess of compound, emphasizing HBX 19,818 binding specificity.

Interestingly, mass shift between unbound and bound USP7 revealed a difference of about −36 Da compared to HBX 19,818 molecular weight (MW; measured mass shift: 386 Da vs. HBX 19,818 average MW: 422 Da), suggesting that part of the molecule and/or the protein is lost upon binding. Moreover, whereas protein/ligand complexes can be usually dissociated using collision-induced dissociation experiments (for review, see Vivat Hannah et al., 2010), USP7/HBX 19,818 complex turned out to be extremely stable in the gas phase (data not shown), raising the hypothesis of a covalent interaction between USP7 and HBX 19,818. This observation was in agreement with dose response of USP7 inhibition showing time-dependent decrease of IC_{50} values as expected for an irreversible inhibitor (Figure 3B). Covalent bonding of HBX 19,818 to USP7 was finally confirmed by MS analysis under denaturing conditions, revealing that USP7/HBX 19,818 complex remains intact after dilution in 50% acetonitrile acidified with 0.5% formic acid (Figure S3A). To gain deeper insights into HBX 19,818 covalent bonding to USP7, reverse-phase liquid chromatography (RPLC) followed by UV and MS detection was used to analyze peptides resulting from trypsin-digested USP7/HBX 19,818 complex (Figure S3B). Comparison of UV chromatogram monitored at $\lambda = 214$ nm (absorbance maximum of peptide bond) and $\lambda = 332$ nm (absorbance maximum of HBX 19,818) revealed two peaks at RT = 44.5 min and RT = 73.1 min absorbing at $\lambda = 332$ nm, which suggests that these peptides carry covalently bound HBX 19,818. Tryptic peptides were then assigned based on their measured MW, which gave rise to 86% sequence coverage, including six out of the seven cysteines (Figure S3C).

To precisely localize the HBX 19,818 binding site in USP7, ligand-bound peptides were submitted to MS/MS experiments. In the case of peptide 218-239, MS/MS spectrum (Figure 3C) displayed numerous fragments providing almost complete sequence coverage. The residue involved in HBX 19,818 covalent bonding was assigned to Cys223; this was evidenced by the 488.2 Da difference between fragments b5 and b6, whereas a 103.0 or 160.0 Da shift would have been expected for a free or alkylated cysteine, respectively. Similarly, for ligand-bound peptide 313-322, MS/MS spectrum revealed that HBX 19,818 is attached to Cys315 (Figure S4A). Based on UV chromatogram ($\lambda = 332$ nm) peak areas (Figure S3B), the abundance ratio of HBX 19,818-bound peptides 218-239 and 313-322 was estimated to 95/5. This result underpins HBX 19,818 selectivity toward Cys223, knowing also that two out of the six other cysteines present in USP7 have side-chain solvent-accessible surface areas 4–5 times higher than Cys223 (Figure S3D). Considering HBX 19,818 molecular formula (Figure 1A), the observed mass increase of 385.2 Da rather than the expected 421.2 Da shift expected from HBX 19,818 monoisotopic mass is explained by HCl release upon covalent bonding (HCl monoisotopic mass: 36.0 Da), as confirmed by high-resolution MS experiments (Figure S4B).

Altogether, combining several MS approaches demonstrated that HBX 19,818 selectively forms a covalent bond with the Cys223 located in the USP7 active site.

To further understand the structural basis of the binding of HBX19,818 to USP7, we carried out molecular docking studies. USP7 has been crystallized in apo-form and together with covalently bound ubiquitin aldehyde (Hu et al., 2002). The observations of the X-ray structures indicate that the active site of the free USP7 core domain exists in an unproductive conformation and that substrate binding will likely trigger a conformational change (catalytic triad in close proximity) that results in catalysis. The docking results show that HBX 19,818 is able to interact with the substrate (ubiquitin) binding pocket of USP7 (Figure S5A). It

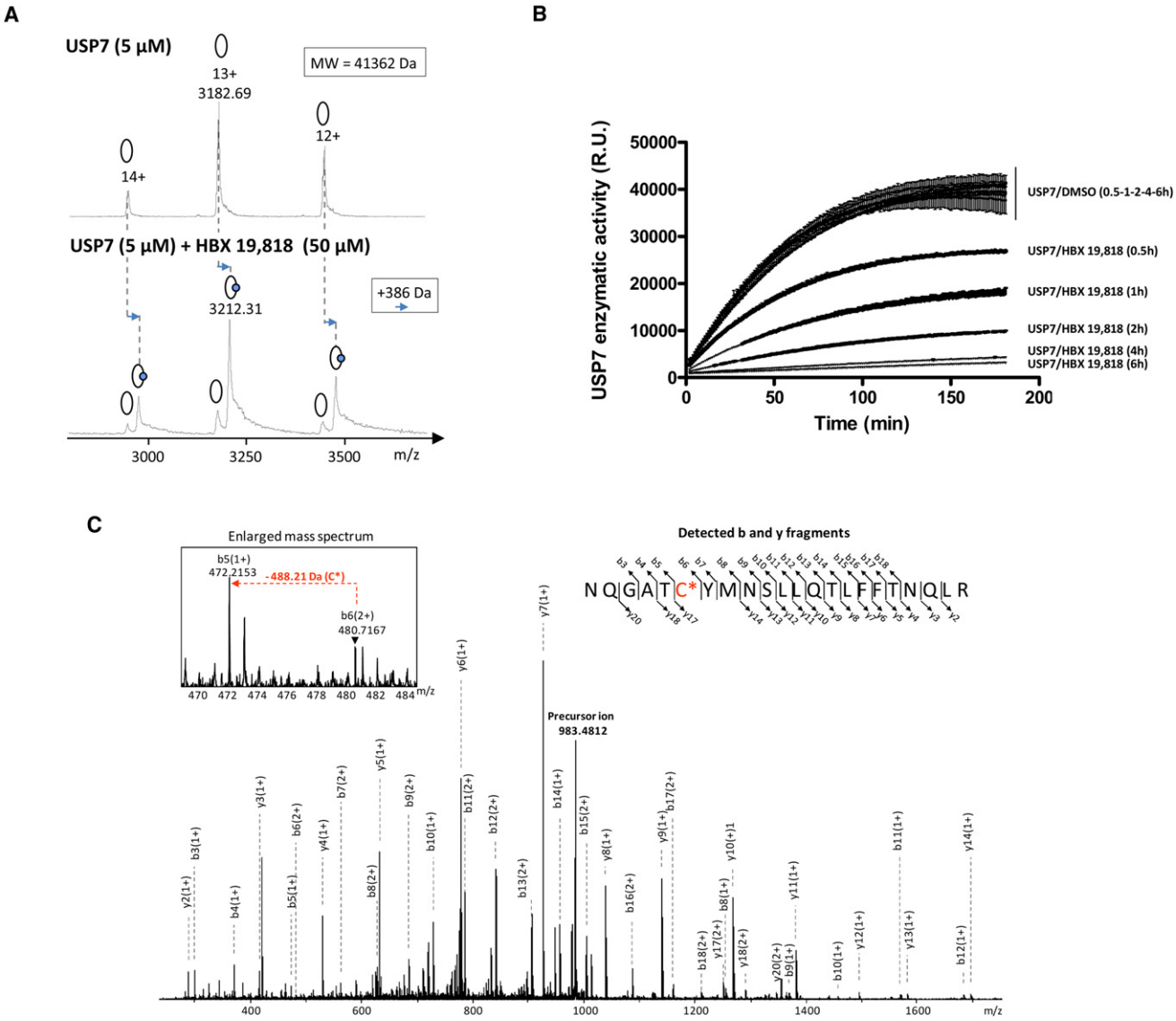

Figure 3. Mode of Action of USP7-Selective Small Molecule Inhibitors

(A) Native MS analysis of USP7 incubated at 5 μM in 10 mM NH_4Ac (pH 7.5) for 15 hr at 18°C either alone (upper mass spectrum) or in the presence of 50 μM HBX 19,818 (lower mass spectrum).

(B) Time-dependent inhibition of USP7 by HBX 19,818. USP7 (100 pM) was pre-incubated for different time points (from 30 min to 6 hr) with DMSO or HBX 19,818 (25 μM) before initiating the enzymatic reaction by adding UbAMC substrate (300 nM).

(C) MS/MS analysis of HBX 19,818-bound peptide 218-239 eluting at 73.6 min in Figure S3B (lower chromatogram).

See also Figures S3, S4, and S5.

shows further that the reactive chloro atom is located nearby the active site Cys223, which enables the formation of a covalent bond between the sulfur atom of Cys223 and the carbon atom bearing the chloro group. This reaction results in the loss of HCl as previously shown in the mass spectrometry study. Further interactions that are observed are strong electrostatic interactions between the basic amino group and two acidic residues (Asp295 and Glu298) located at the entrance of the ubiquitin binding pocket. However, further experimental data, such as crystal structures, are necessary to confirm this docking hypothesis.

HBX 19,818 Selectively Inactivates USP7 in Living Cells

Having demonstrated that HBX 19,818 binds selectively to the active site of USP7 in vitro, we next asked whether HBX 19,818 could inhibit the labeling of USP7 by HAUbVS in living HCT116 cells treated with various amounts of this inhibitor. HBX 19,818 proved to be active in cells, as it almost completely inhibited USP7 labeling at 25 μM (Figure 4A). At this concentration, we also found that HBX 19,818 did not block the labeling of several other DUBs, such as USP8, USP5, USP10, CYLD, or UCH-L3 (Figure 4A). These data clearly demonstrate that HBX 19,818 targets USP7 directly in cells and does not

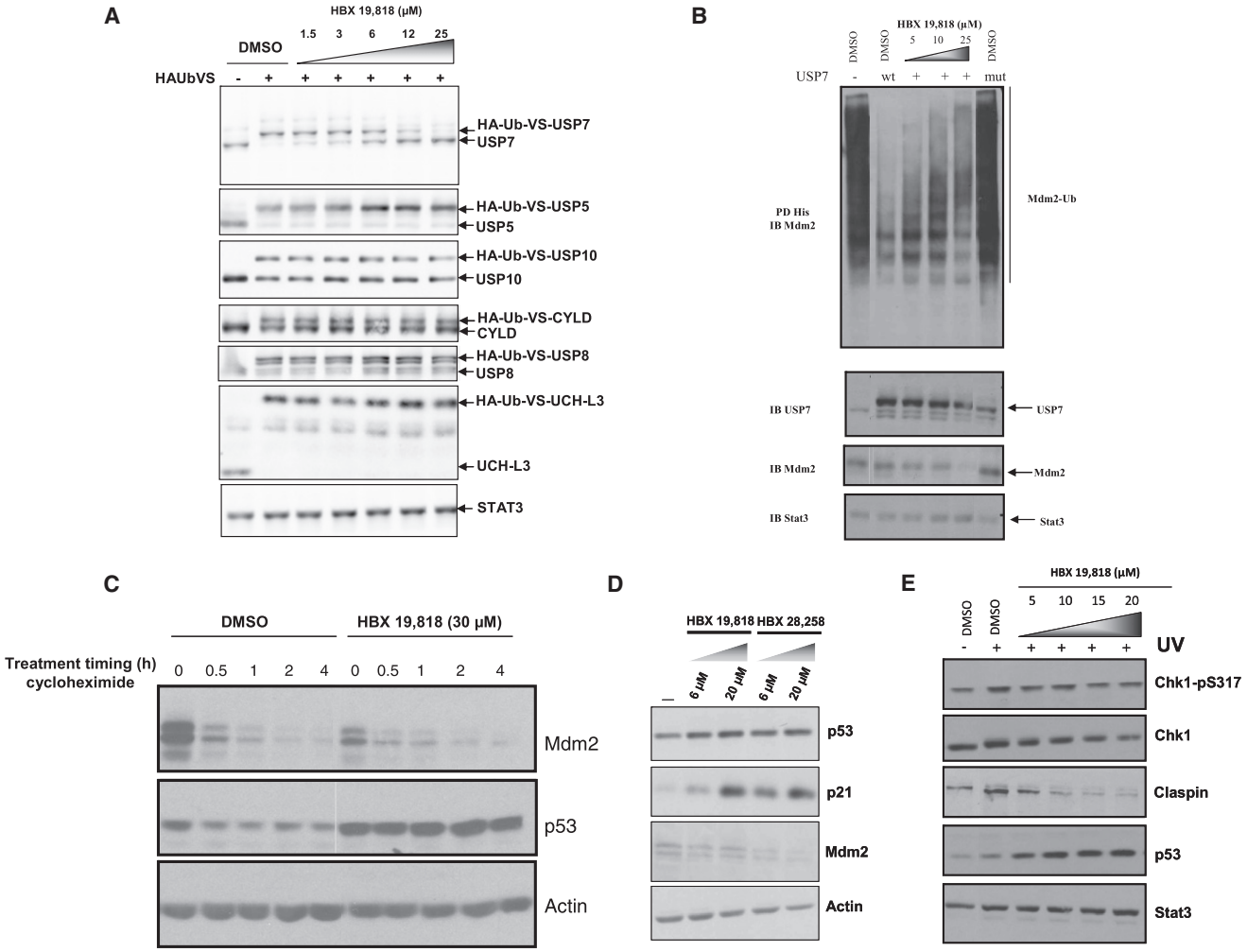

Figure 4. HBX 19,818 Selectively Inhibits USP7 in Human Cancer Cells

(A) Living HCT116 cells treated with HBX 19,818 (1.5, 3, 6, 12, or 25 μM) for 6 hr were then labeled with the HAUbVS probe (1 μM, 15 min). Among the six deubiquitinating enzymes detected by HAUbVS, only USP7 labeling was inhibited by HBX 19,818 (IC_{50} ~6 μM). Individual DUBs were identified using specific antibodies.

(B) Ubiquitinated proteins from HEK293 cells that had been transfected with constructs encoding Mdm2, USP7 (wild-type or inactive C223A mutant), and His-tagged ubiquitin and had been treated with HBX 19,818 (5, 10, or 25 μM) were precipitated using Ni-NTA agarose (PD, pull-down). Western blots were analyzed for the presence of Mdm2 and USP7.

(C) The half-life of endogenous Mdm2 and p53 was monitored in SJSA-1 osteosarcoma cells treated with cycloheximide for different times (0, 0.5, 1, 2, or −4 hr) in the presence of HBX 19,818 (30 μM) for 24 hr. Western blots were analyzed for the presence of Mdm2, p53, and actin.

(D) Endogenous levels of Mdm2, p53, and p21 were monitored in HCT116 colon cancer cells treated with HBX 19,818 or HBX 28,258 (6–20 μM) for 24 hr.

(E) Endogenous levels of claspin, Chk1, Chk1-pS317, and p53 were monitored in U2OS osteosarcoma cells. Cells were treated with HBX 19,818 (5–20 μM) for 24 hr then subsequently treated with UV (10 mJ/cm^2) and harvested 1 hr later. Cells were then processed for immunoblotting.

See also Figure S6.

cross-react with any of the other deubiquitinating enzymes tested.

USP7 stabilizes the product of the well-characterized oncogene, *mdm2*, through specific deubiquitination (Cummins et al., 2004; Li et al., 2004). To confirm that HBX 19,818 inhibits USP7 activity in cells, we developed an assay to monitor the level of the ubiquitinated form of Mdm2 in HEK293 cells. To this end, His-tagged ubiquitin, Mdm2, and USP7 were produced together in HEK293 cells. Ubiquitinated proteins were then pulled down and the polyubiquitinated forms of Mdm2 were detected by immunoblotting with an anti-Mdm2 antibody. In this context, the levels of polyubiquitinated Mdm2 proteins were far lower in the presence of wild-type USP7 than in the presence of the catalytically inactive form of USP7 (Figure 4B, compare lanes 2 and 6), which is consistent with previous reports (Cummins et al., 2004; Li et al., 2004). This assay was used to investigate the effect of HBX 19,818 on USP7-mediated Mdm2 deubiquitination. Incubation of USP7-overproducing HEK293 cells with various amounts of HBX 19,818 for 24 hr resulted in significantly higher levels of Mdm2 polyubiquitinated forms than those in DMSO-treated control cells (Figure 4B, compare lanes 2 and 5). Thus, HBX 19,818 partially reverses the deubiquitination of

Mdm2 by USP7 in HEK293 cells, confirming that HBX 19,818 inhibits a biological activity of USP7 in living cells. We also monitored the level of endogenous Mdm2 in cancer cell lines, such as SJSA-1 osteosarcoma cells that contain an amplified *mdm2* oncogene. In these cancer cells, HBX 19,818 treatment caused a sharp reduction in the steady-state level of endogenous Mdm2, which was accompanied by a strong induction of p53 (Figure 4C, see also Figure S6A for quantification). Incubation of exponentially growing HCT116 cells with HBX 19,818 and HBX 28,258 for 24 hr also led to an increase in the levels of p53 and of the products of its target genes, such as the cyclin-dependent kinase inhibitor $p21^{cip1/waf}$ (Figure 4D, see also Figure S6B for quantification). This result indicated that HBX 19,818 induces the functional activation of p53 in mammalian cells.

Claspin and USP7 interact in vivo, and USP7 is a regulator of claspin stability (Faustrup et al., 2009). As USP7-silencing results in claspin degradation in U2OS osteosarcoma cells, we evaluated whether HBX 19,818 treatment affected the endogenous levels of claspin in these cells. Cells treated for 24 hr exhibited dose-dependent claspin degradation (Figure 4E, see also Figure S6C for quantification). Since claspin is an adaptor protein that facilitates activation of Chk1, a key effector kinase in the DNA damage response, we also monitored the effect of HBX 19,818 on UV-dependent activation of Chk1, as assessed by the level of phosphorylation on its Ser317 residue. As expected, the level of Chk-1 phosphorylation was reduced in HBX 19,818-treated cells. In these conditions, we also detected a dose-dependent accumulation of p53 (Figure 4E). These data taken together indicate that, similar to USP7 knockdown, HBX 19,818 treatment (1) decreases the endogenous level of Phospho-Chk-1, probably as a consequence of lower claspin levels and (2) increases the level of functionally active p53.

Activity of HBX 19,818 on Cell Proliferation, Apoptosis, and Cell Cycle

Since USP7 regulates numerous substrates involved in cell proliferation, we investigated whether HBX 19,818 affected cell proliferation. We treated exponentially growing HCT116 colon cancer cells with various concentrations of HBX 19,818 for 72 hr and then assessed proliferation with BrdU incorporation assays. HBX 19,818 inhibited HCT116 proliferation in a dose-dependent manner, with an IC_{50} of ~2 μM (Figure 5A). To evaluate the role of p53 in the cellular response, cell viability experiments were also performed in three cancer cell lines with different p53 status: HCT116 ($p53^{wt/wt}$), DU145 ($p53^{mt/mt}$), and HeLa (p53 not regulated by Mdm2). Cell viability was affected by HBX 19,818 at a similar level whatever the p53 status (Figure S7), strongly suggesting that p53 seems to play a minor role in the cellular response.

We next evaluated the ability of the USP7 inhibitor to induce apoptosis. We treated HCT116 cells with various concentrations of HBX 19,818, and then assessed the level of apoptosis by assaying caspase-3 activity using a fluorescent substrate or by monitoring poly(ADP-ribose) polymerase (PARP) cleavage. HBX 19,818 was shown to induce HCT116 apoptosis in a dose-dependent manner in both assays (Figure 5B). Given the interaction of USP7 with cell cycle regulators, such as Mel18, claspin, PTEN, FOXO4, and p53, we analyzed the HCT116 cell cycle after HBX 19,818 treatment for 24 hr. Cell cycle analysis revealed that the G1-phase fractions of cells treated with HBX 19,818, but not those of the HBX 28,364-treated cells (a negative control), were significantly greater than those of untreated cells (Figure 5C). Thus, HBX 19,818 treatment, like USP7 knockdown, disrupts cell cycling and leads to G1 arrest.

DISCUSSION

The USP7/HAUSP deubiquitinating enzyme is an attractive viral and oncology target (Colland, 2010). USP7/HAUSP is a cysteine protease, and one of the main problems hindering the development of small-molecule inhibitors of cysteine proteases has been their lack of specificity. However, various DUBs display different tolerances for different residues in their active-site clefts, strongly suggesting that deubiquitinating activity of these different enzymes might be selectively inhibited by small molecules targeting their active sites (Drag et al., 2008). Indeed, specific inhibitors of the viral PLPro and the human USP14 proteasome-associated DUBs were recently identified (Lee et al., 2010; Ratia et al., 2008). The chemical approach to USP7 inhibition we used here led to the identification of small-molecule compounds able to specifically inhibit USP7 in several different assays.

We found that these USP7 inhibitors did not significantly inhibit any of the other deubiquitinating enzymes or the less distantly related cysteine proteases we tested in in vitro enzyme assays of recombinant proteins ($IC_{50} > 200$ μM). Since enzyme behavior can be more complex in cellular contexts, as illustrated with the recent native kinase binding profiles of kinase inhibitors (Patricelli et al., 2011), we used the HAUbVS competitive probe to characterize inhibitor interactions with endogenously expressed deubiquitinating enzymes in a native proteome. This probe was used previously to discover and characterize novel ubiquitin/ubiquitin-like proteases and profile active deubiquitinating enzymes in normal, virus-infected, and malignant cells (Borodovsky et al., 2002; Hemelaar et al., 2004; Ovaa et al., 2004). In these experiments, this class of inhibitors, represented by HBX 19,818 and HBX 28,258, inhibited HAUbVS binding to USP7 with IC_{50} values of 25–50 μM and exhibited excellent selectivity compared to the nonspecific DUB inhibitor HBX 41,108. One specific feature of the USP7 structure is characterized by the different conformation of the catalytic site between the apo-enzyme and the enzyme bound to its natural substrate, ubiquitin (Hu et al., 2002). The marked difference in position between the catalytic residues with and without ubiquitin, observed by superimposition of the two available X-ray structures, is not observed in other pairs of available structures solved with and without ubiquitin (Sippl et al., 2011). Since HBX 19,818 targets the USP7 catalytic site, its selectivity could be linked to this specific structural feature of USP7.

We also showed that these HBX compounds hit the USP7 target, as they disrupted HAUbVS competitive labeling of USP7 in live HCT116 cells. These results demonstrated that the active site of USP7 could be occupied by a small molecule inhibitor in living cells. The specificity of this target occupancy was illustrated by the absence of any off-target activity for HBX 19,818 across several different endogenous deubiquitinating enzymes activities detected in HCT116 cells. In cancer cells,

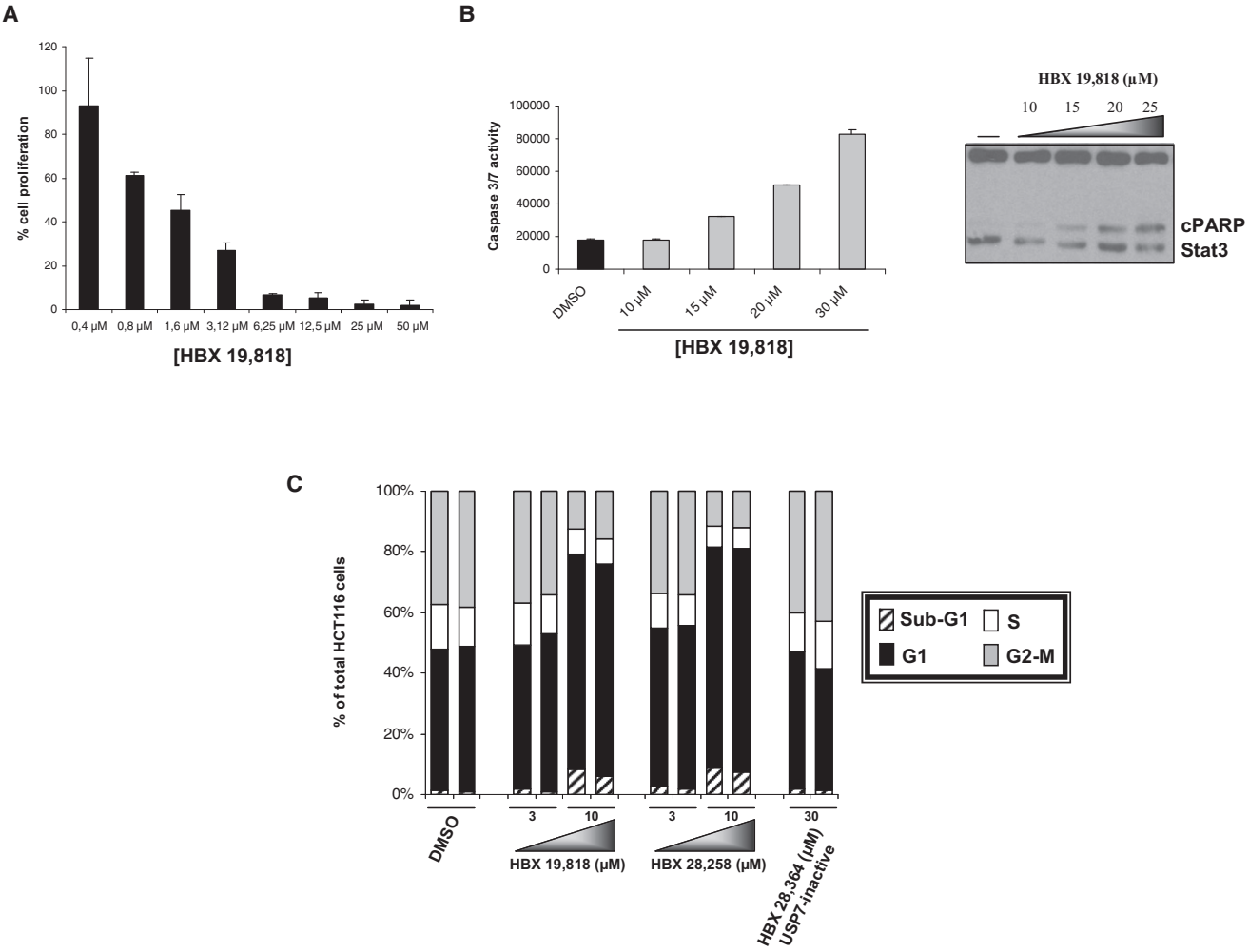

Figure 5. Effect of HBX 19,818 on Cell Proliferation, Apoptosis, and Cell Cycle

(A) Treatment for 72 hr with HBX 19,818 decreased HCT116 cell proliferation in a dose-dependent manner (BrdU incorporation).

(B) Caspase activity was assessed in HCT116 cells following HBX 19,818 treatment (10–30 μM) for 6 hr, using the caspase assay described in the Experimental Procedures. PARP cleavage was detected by western blotting following the treatment of HCT116 cells with HBX 19,818 (10–30 μM) for 6 hr.

(C) HCT116 cells were treated for 24 hr with DMSO, HBX 19,818 (3–10 μM), HBX 28,258 (3–10 μM), or HBX 28,364 (30 μM), and cell cycle profiles were analyzed by fluorescence-activated cell sorting analysis. Cell cycle analysis is presented as a bar chart showing the percentage of cells in subG1, G1, S, and G2-M.

See also Figure S7.

USP7 targeting by HBX 19,818 compromised UV-induced Chk1 phosphorylation and decreased the level of the checkpoint mediator Claspin; both of which occur in response to USP7 knockdown. This targeting was confirmed by the observation that HBX 19,818 modulated the endogenous levels of additional USP7 substrates such as Mdm2 and p53. Regarding Mdm2, we found that higher levels of the ubiquitinated forms of Mdm2 were stabilized by HBX 19,818 treatment and led to Mdm2 degradation, which again resembled USP7 silencing (Sippl et al., 2011). All these data suggest that the observed effects of HBX 19,818 are likely the result of USP7 targeting. Most attempts to target Mdm2 have focused on the identification of small molecules, such as the nutlins, which prevent its interaction with p53 (Vassilev et al., 2004), or on inhibiting its E3 ligase activity (Yang et al., 2005). We adopted an alternative approach based on the identification of small-molecule inhibitors of USP7; an ubiquitin-specific protease required for Mdm2-dependent p53 destabilization. Using HBX 19,818, we found that disrupting USP7 reduced HCT116 cell proliferation, induced caspase activity and PARP cleavage, and arrested HCT116 cancer cells in G1. However, it remains unclear if the mild decrease in endogenous Mdm2 levels observed in response to inhibitor is responsible for upregulation of p53 thus suggesting the involvement of other mediators of p53 induction. Indeed, whereas Mdm2 is sufficient to target p53 for degradation, there is good evidence that it does not function alone. Several proteins, such as transcription factors and E3 ubiquitin ligases, have been shown to be involved in the regulation of p53, and an in-depth characterization of USP7 protein partners in this pathway may help to identify the target effector of USP7 inhibition. In addition, because we observed a minor role of p53 in the cellular response, we cannot exclude that USP7 regulates the function

of a known or not yet known substrate involved in cell death or that HBX 19,818 has additional off-target, p53-independent proapoptotic effects.

These compounds were shown to be irreversible inhibitors of USP7 through nucleophilic attack of its catalytic cysteine, resulting in chloride release and covalent binding. Molecular docking hypotheses based on the structure of the ubiquitin-bound USP7 core are consistent with such a mechanism. This irreversible mechanism of action for HBX 19,818 is supported by our competitive HAUbVS results showing that inhibition of USP7 was sustained in cellular extracts of HBX 19,818-treated HCT116 cells. Assuming that HBX 19,818 is an irreversible inhibitor, evaluation of USP7 target occupancy in animal models could be envisaged, as previously described for irreversible hydrolase inhibitors (Chang et al., 2011). This would allow the extent and duration of USP7 target inhibition to be determined as well as its relationship to antitumor activity, an important parameter in a drug discovery process. Future experiments with these covalent inhibitors could also include their use as powerful tools for defining the binding site for reversible inhibitors on USP7 enzyme molecules and their use as probes by incorporating a fluorophore into the HBX 19,818 structure to image USP7 activity in vivo.

There is increasing evidence to suggest that DUB inhibition is potentially useful for the treatment of viral disease, neurological disorders and cancer treatment. This study provides proof-of-principle that specific cell-permeable inhibitors of USP7, a critical oncology target, can be identified. Further structure-activity relationships and protein structural studies will be required to assess the potential for USP7 inhibitors as therapeutics in cancer. These inhibitors can also be valuable tools for studying USP7-mediated deubiquitination.

SIGNIFICANCE

Regulated protein turnover is primarily controlled by the ubiquitin-proteasome system. Ubiquitin-specific proteases are involved in the deubiquitination of specific target substrates regulating their stability, subcellular localization and/or activation status. The strong connection of USPs with cancer phenotypes clearly highlights these proteins as attractive candidates for cancer drug discovery. The human USP7 deubiquitinating enzyme appears as such a strategic target for cancer therapy since it regulates many proteins involved in the cell cycle, as well as tumor suppressors and oncogenes. One of the most acute challenges in developing cysteine protease inhibitors with lead-like properties is selectivity. This could predictably be an issue with USPs as they constitute the largest family of human cysteine proteases, gathering more than 60 different members. Specific inhibitors of the viral PLPro and the human USP14 proteasome-associated deubiquitinating enzymes were recently identified. In this work we discovered specific and cell-active inhibitors of the USP7 deubiquitinating enzyme using biochemical assays and activity-based protein profiling in living systems. The therapeutic potential of inhibiting USP7 was demonstrated by the observation that these inhibitors can bind directly and specifically to USP7 and modulate the steady-state levels of several USP7 substrates. The current USP7 inhibitors also can be a valuable chemical tool for studying USP7-mediated deubiquitination.

EXPERIMENTAL PROCEDURES

Protein Production and Purification

Full-length wild-type and catalytic mutant (cysteine 223 replaced by alanine, C223A) human His-USP7 proteins, as well as full-length wild-type human His-USP8, were produced in *Spodoptera frugiperda* cells (Sf9; Invitrogen, Carlsbad, CA, USA) using the Bac-to-Bac baculovirus system from Invitrogen in accordance with the manufacturer's instructions and purified as previously described (Colland et al., 2009). Recombinant SENP1 (E-700), USP2 (E-506), USP5 (E-322), USP20 (E-344), UCH-L1 (E-340), and UCH-L3 (E-325) proteins were provided by Boston Biochem (Cambridge, MA, USA). Cathepsin B and caspase-3 were provided by Calbiochem (219364; Darmstadt, Germany) and BD Biosciences (556472; Franklin Lakes, NJ, USA), respectively.

HTS Screening

Deubiquitinating enzyme activity was monitored in a fluorometric assay, using ubiquitin-AMC (ubiquitin-7-amido-4-methylcoumarin, Boston Biochem, U-550) as a substrate (Dang et al., 1998). USP7 has been shown to catalyze Ub-AMC hydrolysis. The AMC released from the C terminus of ubiquitin displays enhanced fluorescence, which can be monitored with a fluorescence reader. USP7 inhibitors were identified by screening a proprietary library of 36,000 chemically diverse compounds (Monge et al., 2006) for inhibition of the enzyme-mediated cleavage of the AMC fluorophore from ubiquitin-AMC. HTS assays were performed using a Perkin Elmer (Waltham, MA, USA) Janus automated liquid handler and a 384-well format (Greiner black plates). Both enzyme and substrate were freshly prepared in USP7 reaction buffer (50 mM Tris-HCl [pH 7.6], 0.5 mM EDTA, 5 mM DTT, 0.01% Triton X-100, and 0.05 mg/ml serum albumin) for each run. USP7 (100 pM) were pre-incubated with DMSO (5%) or compounds (10 μM) for 30 min, and the enzymatic reaction was initiated by adding the UbAMC substrate (300 nM). The reaction mixture was incubated at room temperature for 1 hr, and the reaction was stopped by adding acetic acid (100 mM). Fluorescence emission intensity was measured on a PHERAstar (BMG Labtech, Ortenberg, Germany) machine, using a coumarin filter set (λ_{ex} = 360 nm, λ_{em} = 460 nm). The Z' factor, a standard statistical parameter for HTS assays, was 0.92, indicative of a robust HTS assay (>0.5; Zhang et al., 1999).

Cysteine Protease Fluorogenic Substrate Activity Assay

The ability of HBX 19,818 and HBX 28,258 to inhibit a panel of deubiquitinating enzymes, including UCH-L3 (13 pM), USP7 (100 pM), USP8 (1.36 nM), UCH-L1 (2.5 nM), USP5 (10 nM), USP20 (10 nM), and USP2 (500 pM), was tested using the UbAMC substrate (300 nM). The potential effects of HBX 19,818 and HBX 28,258 were also tested on the enzymatic activities of SENP1 (80 pM), cathepsin-B (100 pM), and caspase-3 (100 pM) using the SUMO1-AMC (750 nM), ZRR-AMC (3 μM), and DEVD-AMC (250 nM) substrates, respectively. All enzymes were tested in USP7 reaction buffer (50 mM Tris-HCl [pH 7.6], 0.5 mM EDTA, 5 mM DTT, 0.01% Triton X-100, and 0.05 mg/ml serum albumin), except for two enzymes, USP8 (same buffer but pH 8.8) and caspase-3 (100 mM HEPES [pH 7.5], 10% sucrose, and 0.1% CHAPS). All enzymes were pre-incubated with DMSO or compounds for 30 min at room temperature, and the enzymatic reaction was initiated by adding the substrate of interest. The reaction mixture was incubated at room temperature for 1 hr, and the reaction was stopped by adding acetic acid (100 mM). The reactions were monitored using the PHERAstar (BMG Labtech).

Mass Spectrometry

Prior to MS experiments, detagged USP7 was buffer exchanged against 50 mM ammonium acetate (pH 7.5). For compound binding analysis by native MS, protein (5 μM) was incubated overnight at 18°C in 10 mM ammonium acetate (pH 7.5) in the presence of increasing compound concentrations (5 to 50 μM). Denaturing mass spectra of USP7/HBX 19,818 complex were obtained after 5-fold dilution of protein/ligand mixtures in 50% acetonitrile/0.5% formic acid. For a peptide mapping experiment, trypsin-digested USP7/HBX 19,818 covalent complex was analyzed by reverse-phase liquid

chromatography (RPLC) coupled to UV and MS detection. Ligand-bound peptides were collected after RPLC separation and submitted to high-resolution MS and MS/MS experiments. Additional details regarding MS experiments are given in the Supplemental Experimental Procedures.

Labeling and Competition for Deubiquitinating Activity with the HAUbVS Activity-Based Probe

HCT116, as well as HEK293, cells were harvested and lysed on ice with a nondenaturing buffer containing 50 mM Tris [pH 7.4], 150 mM NaCl, 5 mM $MgCl_2$, 0.5 mM EDTA, 2 mM DTT, 2 mM ATP, 0.5% NP40, and 10% glycerol. Proteins from nondenatured cell lysates (50 μg) were treated with compounds of interest for 2 hr at room temperature. The ubiquitin labeling reaction was initiated by adding HAUbVS (to a final concentration of 1 μM) in labeling buffer (50 mM Tris [pH 7.6], 5 mM $MgCl_2$; 0.5 mM EDTA, 2 mM DTT, 2 mM ATP and 250 mM sucrose), and the reaction was allowed to proceed in a final volume of 30 μl at room temperature for 15 min. To evaluate drug occupancy on USP7 in cells, living HCT116 cells were also directly treated with HBX 19,818 compound for 6 hr, harvested, and lysed on ice in the nondenaturing buffer described previously. Samples were incubated at 4°C for 1 hr, briefly sonicated, and clarified. Proteins were then quantified using bicinchoninic acid (Sigma-Aldrich, St. Louis, MO, USA). The ubiquitin labeling reaction was initiated by adding 0.3 μg HAUbVS to 50 μg of proteins from nondenatured cell lysates. The reaction was allowed to proceed at room temperature for 15 min. Samples were then heated at 100°C for 5 min, briefly sonicated, and processed for immunoblotting as described in the Western Blot Experiments paragraph.

Cell Culture Analysis

Human embryo kidney HEK293 cells (European Cell Culture Collection) were maintained in Dulbecco's modified Eagle's medium, supplemented with 10% FBS, 2 mM glutamine, 1 mM sodium pyruvate, and 1% nonessential amino acids. Human colon carcinoma HCT116 cells were maintained in McCoy's 5A medium, supplemented with 10% FBS and 3 mM glutamine. Human osteosarcoma U2OS cells (European Cell Culture Collection) were maintained in Mc Coys' 5A medium, supplemented with 10% FBS and 1.6 mM glutamine. Human osteosarcoma SJSA-1 cells (American Type Culture Collection) were maintained in RPMI 1640 medium, supplemented with 10% FBS, 2 mM glutamine, 10 mM HEPES, and 2.4 g/l glucose. All culture media were supplemented with 100 units/ml penicillin and 0.1 mg/ml streptomycin, and cell lines were cultured at 37°C in a humidified atmosphere containing 5% CO_2. Following compound treatment for the indicated time at the indicated concentrations, cells were always washed once in PBS and harvested by treatment with trypsin. Cell proliferation, apoptosis, and cell cycle studies are described in the Supplemental Experimental Procedures.

Western Blot Experiments

Following HBX 19,818 treatment for the indicated time at the indicated concentrations, cells were washed once in PBS and harvested by treatment with trypsin. Detached and trypsin-treated cells were pooled and collected by centrifugation. Cells were then resuspended in lysis buffer (2% SDS supplemented in 1X protease inhibitor cocktail; Sigma-Aldrich), heated for 10 min at 100°C, and briefly sonicated. Proteins were quantified using bicinchoninic acid (Sigma-Aldrich) in accordance with the manufacturer's instructions and resolved by sodium dodecyl sulfate polyacrylamide gel electrophoresis (SDS-PAGE). Separated proteins were transferred to a nitrocellulose membrane and probed with antibodies against p53 (DO-1; Santa Cruz; sc-126), p21 (BD PharMingen; 556430), PARP (Cell Signaling, Danvers, MA, USA; 9542), Mdm2 (SMP14; Santa Cruz; sc-965), HA (BabCO; MMS-101P), USP7 (Calbiochem; DR1014), USP5 (Bethyl Lab; A301-542A), USP10 (Epitomics; 3148-1), CYLD (Santa Cruz; sc-137139), USP8 (Sigma-Aldrich; HPA004869), UCH-L3 (Cell Signaling; 3525S), caspase-3 (Cell Signaling; 9661), phospho-S317-Chk1 (Cell Signaling; 2344S), Chk1 (Santa Cruz; sc-8408), Claspin (Bethyl Lab; A300-266A), stat3 (Cell Signaling; 9132), and actin (Sigma-Aldrich; A2066). Horseradish peroxidase (HRP)-conjugated anti-mouse (Jackson Laboratories, Bar Habor, ME, USA; 115-035-003) or HRP-conjugated anti-rabbit (Cell Signaling; 7074) antibodies were used as secondary antibodies. Signals were detected by enhanced chemiluminescence (Pierce ECL or Amersham ECL Advance) in accordance with the reagent manufacturer's instructions.

Deubiquitination Assays

HEK293 cells were transfected with the constructs indicated. Forty hours after transfection, cells were treated for 24 hr with various concentrations of HBX 19,818 and lysed in urea lysis buffer (0.1 M sodium phosphate [pH 8.0], 10 mM Tris-HCl [pH 8.0], 300 mM NaCl, 8 M urea, 0.1% Triton X-100, and 20 mM imidazole). Ubiquitinated proteins were precipitated from urea lysates, using Ni-NTA agarose beads (Qiagen, Germantown, MD, USA), essentially as described previously (van der Horst et al., 2006), and analyzed by western blotting for the presence of Mdm2. For the in vitro deubiquitination of p53 by USP7, the purified enzyme (3 nM final concentration) was incubated with HBX 19,818 at the indicated concentration for 30 min at room temperature before the addition of purified p53 that had been polyubiquitinated by Mdm2 (kindly provided by O. Coux). Reactions were incubated for 90 min at 37°C and stopped by adding denaturing 1X NuPAGE LDS Sample Buffer (Invitrogen) and 0.1 M DTT (final concentration). Samples were resolved by SDS-PAGE, and the separated proteins were then transferred to a nitrocellulose membrane and probed with anti-p53 antibody (DO-1; Santa Cruz; sc-126).

SUPPLEMENTAL INFORMATION

Supplemental Information includes seven figures and Supplemental Experimental Procedures and can be found with this article online at doi:10.1016/j.chembiol.2012.02.007.

ACKNOWLEDGMENTS

We wish to thank all the staff of Hybrigenics for contributing to this study. We wish to thank Olivier Coux for providing the ubiquitinated p53 substrate. We also thank Marie-Edith Gourdel, Rémi Delansorne, and François Bellamy for many stimulating discussions.

Received: December 5, 2011
Revised: January 31, 2012
Accepted: February 13, 2012
Published: April 19, 2012

REFERENCES

Altun, M., Kramer, H.B., Willems, L.I., McDermott, J.L., Leach, C.A., Goldenberg, S.J., Kumar, K.G., Konietzny, R., Fischer, R., Kogan, E., et al. (2011). Activity-based chemical proteomics accelerates inhibitor development for deubiquitylating enzymes. Chem. Biol. *18*, 1401–1412.

Becker, K., Marchenko, N.D., Palacios, G., and Moll, U.M. (2008). A role of HAUSP in tumor suppression in a human colon carcinoma xenograft model. Cell Cycle *7*, 7–10.

Borodovsky, A., Ovaa, H., Kolli, N., Gan-Erdene, T., Wilkinson, K.D., Ploegh, H.L., and Kessler, B.M. (2002). Chemistry-based functional proteomics reveals novel members of the deubiquitinating enzyme family. Chem. Biol. *9*, 1149–1159.

Chang, J.W., Nomura, D.K., and Cravatt, B.F. (2011). A potent and selective inhibitor of KIAA1363/AADACL1 that impairs prostate cancer pathogenesis. Chem. Biol. *18*, 476–484.

Chen, J., Dexheimer, T.S., Ai, Y., Liang, Q., Villamil, M.A., Inglese, J., Maloney, D.J., Jadhav, A., Simeonov, A., and Zhuang, Z. (2011). Selective and cell-active inhibitors of the USP1/ UAF1 deubiquitinase complex reverse cisplatin resistance in non-small cell lung cancer cells. Chem. Biol. *18*, 1390–1400.

Cohen, P., and Tcherpakov, M. (2010). Will the ubiquitin system furnish as many drug targets as protein kinases? Cell *143*, 686–693.

Colland, F., Formstecher, E., Jacq, X., Reverdy, C., Planquette, C., Conrath, S., Trouplin, V., Bianchi, J., Aushev, V.N., Camonis, J., et al. (2009). Small-molecule inhibitor of USP7/HAUSP ubiquitin protease stabilizes and activates p53 in cells. Mol. Cancer Ther. *8*, 2286–2295.

Colland, F. (2010). The therapeutic potential of deubiquitinating enzyme inhibitors. Biochem. Soc. Trans. *38*, 137–143.

Cummins, J.M., Rago, C., Kohli, M., Kinzler, K.W., Lengauer, C., and Vogelstein, B. (2004). Tumour suppression: disruption of HAUSP gene stabilizes p53. Nature *428*. 10.1038/nature02501.

Dang, L.C., Melandri, F.D., and Stein, R.L. (1998). Kinetic and mechanistic studies on the hydrolysis of ubiquitin C-terminal 7-amido-4-methylcoumarin by deubiquitinating enzymes. Biochemistry *37*, 1868–1879.

Drag, M., and Salvesen, G.S. (2010). Emerging principles in protease-based drug discovery. Nat. Rev. Drug Discov. *9*, 690–701.

Drag, M., Mikolajczyk, J., Bekes, M., Reyes-Turcu, F.E., Ellman, J.A., Wilkinson, K.D., and Salvesen, G.S. (2008). Positional-scanning fluorigenic substrate libraries reveal unexpected specificity determinants of DUBs (deubiquitinating enzymes). Biochem. J. *415*, 367–375.

Du, Z., Song, J., Wang, Y., Zhao, Y., Guda, K., Yang, S., Kao, H.Y., Xu, Y., Willis, J., Markowitz, S.D., et al. (2010). DNMT1 stability is regulated by proteins coordinating deubiquitination and acetylation-driven ubiquitination. Sci. Signal. *3*, ra80.

Epping, M.T., Meijer, L.A., Krijgsman, O., Bos, J.L., Pandolfi, P.P., and Bernards, R. (2011). TSPYL5 suppresses p53 levels and function by physical interaction with USP7. Nat. Cell Biol. *13*, 102–108.

Everett, R.D., Meredith, M., and Orr, A. (1999). The ability of herpes simplex virus type 1 immediate-early protein Vmw110 to bind to a ubiquitin-specific protease contributes to its roles in the activation of gene expression and stimulation of virus replication. J. Virol. *73*, 417–426.

Faesen, A.C., Dirac, A.M., Shanmugham, A., Ovaa, H., Perrakis, A., and Sixma, T.K. (2011). Mechanism of USP7/HAUSP activation by its C-terminal ubiquitin-like domain and allosteric regulation by GMP-synthetase. Mol. Cell *44*, 147–159.

Faustrup, H., Bekker-Jensen, S., Bartek, J., Lukas, J., and Mailand, N. (2009). USP7 counteracts SCFbetaTrCP- but not APCCdh1-mediated proteolysis of Claspin. J. Cell Biol. *184*, 13–19.

Hemelaar, J., Borodovsky, A., Kessler, B.M., Reverter, D., Cook, J., Kolli, N., Gan-Erdene, T., Wilkinson, K.D., Gill, G., Lima, C.D., et al. (2004). Specific and covalent targeting of conjugating and deconjugating enzymes of ubiquitin-like proteins. Mol. Cell. Biol. *24*, 84–95.

Hu, M., Li, P., Li, M., Li, W., Yao, T., Wu, J.W., Gu, W., Cohen, R.E., and Shi, Y. (2002). Crystal structure of a UBP-family deubiquitinating enzyme in isolation and in complex with ubiquitin aldehyde. Cell *111*, 1041–1054.

Komander, D., Clague, M.J., and Urbé, S. (2009). Breaking the chains: structure and function of the deubiquitinases. Nat. Rev. Mol. Cell Biol. *10*, 550–563.

Lee, B.H., Lee, M.J., Park, S., Oh, D.C., Elsasser, S., Chen, P.C., Gartner, C., Dimova, N., Hanna, J., Gygi, S.P., et al. (2010). Enhancement of proteasome activity by a small-molecule inhibitor of USP14. Nature *467*, 179–184.

Li, M., Brooks, C.L., Kon, N., and Gu, W. (2004). A dynamic role of HAUSP in the p53-Mdm2 pathway. Mol. Cell *13*, 879–886.

Maertens, G.N., El Messaoudi-Aubert, S., Elderkin, S., Hiom, K., and Peters, G. (2010). Ubiquitin-specific proteases 7 and 11 modulate Polycomb regulation of the INK4a tumour suppressor. EMBO J. *29*, 2553–2565.

Monge, A., Arrault, A., Marot, C., and Morin-Allory, L. (2006). Managing, profiling and analyzing a library of 2.6 million compounds gathered from 32 chemical providers. Mol. Divers. *10*, 389–403.

Muratani, M., Gerlich, D., Janicki, S.M., Gebhard, M., Eils, R., and Spector, D.L. (2002). Metabolic-energy-dependent movement of PML bodies within the mammalian cell nucleus. Nat. Cell Biol. *4*, 106–110.

Nijman, S.M., Luna-Vargas, M.P., Velds, A., Brummelkamp, T.R., Dirac, A.M., Sixma, T.K., and Bernards, R. (2005). A genomic and functional inventory of deubiquitinating enzymes. Cell *123*, 773–786.

Ovaa, H., Kessler, B.M., Rolén, U., Galardy, P.J., Ploegh, H.L., and Masucci, M.G. (2004). Activity-based ubiquitin-specific protease (USP) profiling of virus-infected and malignant human cells. Proc. Natl. Acad. Sci. USA *101*, 2253–2258.

Patricelli, M.P., Nomanbhoy, T.K., Wu, J., Brown, H., Zhou, D., Zhang, J., Jagannathan, S., Aban, A., Okerberg, E., Herring, C., et al. (2011). In situ kinase profiling reveals functionally relevant properties of native kinases. Chem. Biol. *18*, 699–710.

Ratia, K., Pegan, S., Takayama, J., Sleeman, K., Coughlin, M., Baliji, S., Chaudhuri, R., Fu, W., Prabhakar, B.S., Johnson, M.E., et al. (2008). A noncovalent class of papain-like protease/deubiquitinase inhibitors blocks SARS virus replication. Proc. Natl. Acad. Sci. USA *105*, 16119–16124.

Sippl, W., Collura, V., and Colland, F. (2011). Ubiquitin-specific proteases as cancer drug targets. Future Oncol. *7*, 619–632.

Song, M.S., Salmena, L., Carracedo, A., Egia, A., Lo-Coco, F., Teruya-Feldstein, J., and Pandolfi, P.P. (2008). The deubiquitinylation and localization of PTEN are regulated by a HAUSP-PML network. Nature *455*, 813–817.

van der Horst, A., de Vries-Smits, A.M., Brenkman, A.B., van Triest, M.H., van den Broek, N., Colland, F., Maurice, M.M., and Burgering, B.M. (2006). FOXO4 transcriptional activity is regulated by monoubiquitination and USP7/HAUSP. Nat. Cell Biol. *8*, 1064–1073.

Vassilev, L.T., Vu, B.T., Graves, B., Carvajal, D., Podlaski, F., Filipovic, Z., Kong, N., Kammlott, U., Lukacs, C., Klein, C., et al. (2004). In vivo activation of the p53 pathway by small-molecule antagonists of MDM2. Science *303*, 844–848.

Vivat Hannah, V., Atmanene, C., Zeyer, D., Van Dorsselaer, A., and Sanglier-Cianférani, S. (2010). Native MS: an 'ESI' way to support structure- and fragment-based drug discovery. Future Med. Chem *2*, 35–50.

Yang, Y., Ludwig, R.L., Jensen, J.P., Pierre, S.A., Medaglia, M.V., Davydov, I.V., Safiran, Y.J., Oberoi, P., Kenten, J.H., Phillips, A.C., et al. (2005). Small molecule inhibitors of HDM2 ubiquitin ligase activity stabilize and activate p53 in cells. Cancer Cell *7*, 547–559.

Zapata, J.M., Pawlowski, K., Haas, E., Ware, C.F., Godzik, A., and Reed, J.C. (2001). A diverse family of proteins containing tumor necrosis factor receptor-associated factor domains. J. Biol. Chem. *276*, 24242–24252.

Zhang, J.H., Chung, T.D., and Oldenburg, K.R. (1999). A simple statistical parameter for use in evaluation and validation of high throughput screening assays. J. Biomol. Screen. *4*, 67–73.